Available at https://journalenrichment.com/index.php/jr/

Enrichment: Journal of Multidisciplinary Research and Development

ANALYSIS OF CTD PARAMETERS IN BAWEAN WATERS USING 3D MODELING

Avly Arfiani Khoirunnisaa*, La Ode Alam Minsaris[1], Ayang Armelita Rosalia[1], Nadia Zahrina Wulansari[2]
Universitas Pendidikan Indonesia, Indonesia
Email: avlyarfiani@upi.edu

ABSTRACT

Bawean waters, located in the Java Sea about 150 km north of Gresik, East Java Province, have complex oceanographic characteristics that are interesting to study. The biodiversity and oceanographic conditions of its waters are influenced by hydrodynamic factors, such as ocean currents, tides, and other physical and chemical parameters. This study aims to analyze the oceanographic characteristics of the waters around Bawean Island based on the parameters of temperature, salinity, density, conductivity, and sound speed that play a role in the dynamics of the water mass. Measurements were made using CTD (Conductivity, Temperature, and Depth) instruments with the Direct Reading method, which allows real-time analysis of water masses. The data obtained was then processed using Ocean Data View (ODV) software to identify the distribution patterns of oceanographic parameters. In addition, Surfer software was used in modeling the three-dimensional visualization of oceanographic parameter density distribution patterns. The study sites were categorized into three zones, namely near land, far land, and perpendicular to land, to understand the differences in parameter distribution in different areas. The results showed that the water temperature was in the range of 28.75°C-31.25°C, salinity 26-33.1 PSU, conductivity 45-55 µS/cm, density 1016-1021 kg/m^3, and sound speed 1534-1543 m/s. The modeling results and contour maps show that there is a connected density distribution pattern from the causation of low temperature parameters that affect the increase in salinity, conductivity, density, and decrease in sound speed. In addition, this research is expected to provide an in-depth understanding of the distribution patterns, distribution of oceanographic parameters in the waters of Bawean Island and the influence of factors that affect them.

Keywords; Bawean Waters, CTD, Modeling, ODV, Surfer

INTRODUCTION

Bawean Island is located in the Java Sea, approximately 150km north of Gresik, East Java Province. The island with an area of about 196.27 km^2, which consists of two sub-districts, namely Sangkapura Sub-district and Tambak Sub-district, is often dubbed as "Hidden Paradise" because it has stunning waters, such as clear sea water, white sandy beaches, and biodiversity (Mutmainnah et al. 2021). This rich biodiversity and oceanographic conditions make it an attractive object for scientific research, especially in the field of oceanography. Mutmainnah, et.al, 2021, said the oceanographic characteristics in Bawean waters are influenced by the dynamics of ocean currents, tides, and other physical and chemical parameters. In research Djumanto, 2010, it was also stated that Bawean waters have an important role in the Java Sea ecosystem, which is a migration route for various marine species. According to Lubis et.al, 2018, the oceanographic conditions of a body of water can affect the sustainability of the surrounding marine ecosystem and contribute to global environmental change. Thus, a study of the oceanographic characteristics of this location's water mass is needed.

The interest in studying the waters around Bawean is based on the importance of understanding the oceanographic dynamics in the region. The parameter as measured data are temperature, salinity, density, conductivity, and sound speed. These parameters generally play an important role in distribution patterns, nutrient distribution, and air mass movement (Yuliardi, et.al, 2022). Modern oceanographic instruments, such as CTD (Conductivity, Temperature, and Depth) are the main tools in research, as stated by Herwindya et al. 2020, that CTD measurements are used to analyze the water mass characteristics of a water body and also as an input for accurate and real-time bathymetry survey corrections. According to Williams. A.J, 2009, also stated that one of the most useful instruments developed to determine seawater properties over the past four decades is CTD. CTD data is then processed using ODV (Ocean Data View) software to see the distribution pattern of oceanographic parameter distribution based on depth. To support detailed analysis results, in this study the location of parameter distribution is categorized into three types, namely near land, far land and perpendicular to land. This is done so that researchers can analyze comparisons of differences in parameter distribution patterns at each different angle.

In addition to ODV, data processing was also developed using Surfer software to visualize the density distribution model in the form of three-dimensional (3D) contour maps. Based on a statement from Soesanto et al. 2022, it is explained that Surfer software is a development of underwater technology that is used for 3D modeling simulations, making bathymetry contour maps, modeling sediment layers, or other interpretation needs. So, this research utilizes Surfer in the analysis of parameter distribution patterns, because Surfer software has outputs that are in accordance with the needs as well as introducing it to the general public.

The final results of the research are expected to provide a more comprehensive understanding of the oceanographic characteristics in Bawean waters in the form of the results of the distribution of temperature, salinity, conductivity, density and sound speed parameters in the form of horizontal and vertical distribution using ODV. In addition, this research can also provide interpretation of modeling done using Surfer. Through this research, hopefully it can be applied to the development of other oceanographic study needs.

METHOD

This research was conducted with a type of documentary research or desk research, which is one type of research by analyzing case studies from survey data, documents, reports and other archives that do not require the author to participate in the field directly, but the data obtained is still data from the field as the type of research conducted (Mangarin, et.al, 2024). Researchers obtained data from the Pusat Hidro-Oseanografi TNI AL based on the activities of the Hydro-Oceanographic Survey and Mapping Operation (Opssurta Hidros) which is part of the Pushidrosal team survey in March 2019 with the research focus on the Java Sea Waters Segment 5, Bawean Island with the time zone GMT+7 and Datum WGS 84 (Pushidrosal, 2019). The research location in this paper is divided into 10 station points which are then analyzed in the form of 3 pull patterns or station line groupings as presented in Figure 1.

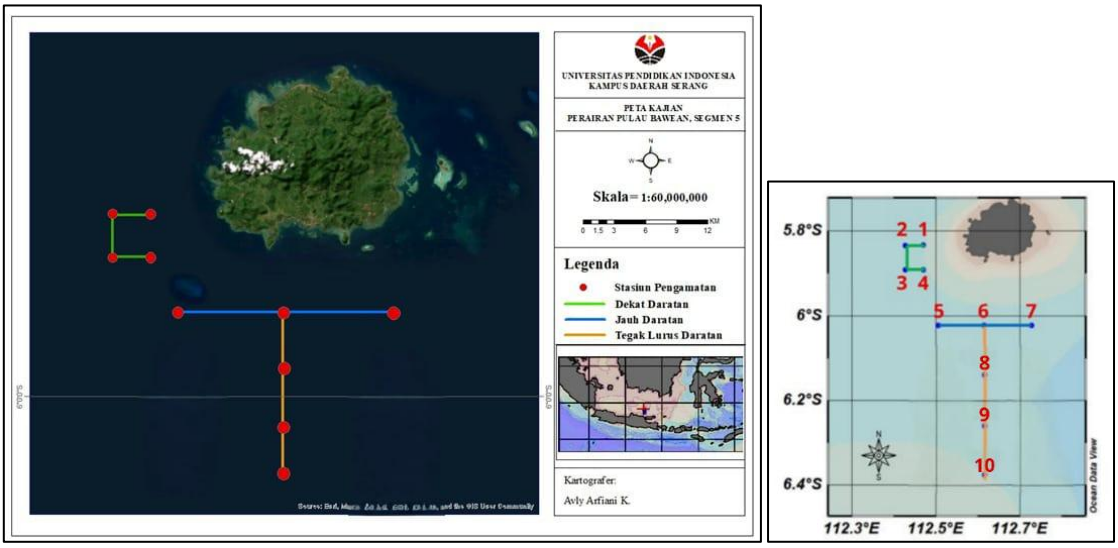

Figure 1. Author's Observation Legend Map
(Source: Author, 2025)

In Figure 1. is the author's research location, where the green line is the station group near the mainland, the blue line is the station group far from the mainland and the orange line is the station group perpendicular to the mainland. This is done to be able to see how the results of the comparison of the distribution of ODV-based oceanographic parameters based on their location with reference to land. The research location point was carried out in the northern waters of the Java Sea Segment 5, Bawean Island with coordinates 06°30'37.2897" LS - 112°49'32.1630" BT using Visual GPS View software right at reference point HP.130048 for position control center (Pushidrosal, 2019).

CTD data collection methods are carried out simultaneously and systematically, as visualized in the attached figures in Figure 2 below.

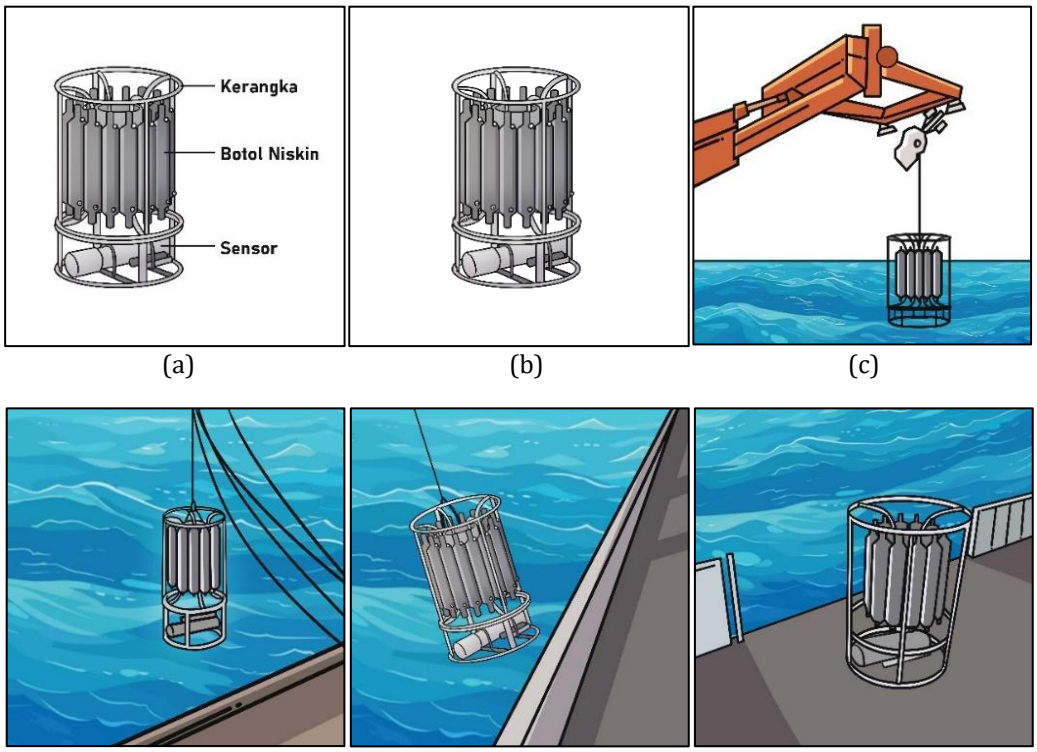

Figure 2. How CTD Usage Works (a=CTD chart, b=step 1, c=step 2, d=step 3, e=step 4 and e=step 5)
(Source: Author, 2025)

Methods are divided into two types, namely data collection methods and research methods for data processing results. The illustration above explains the steps taken when collecting data using the CTD tool. Figure 2 (a) visualizes the main chart of the CTD, namely the frame as the foundation, the niskin bottle as a water sample storage device, and the sensor machine circuit as a measuring instrument of oceanographic parameters. Figure (b) shows the initial stage of the research, where the CTD device has to be prepared and checked to be ready for use. Before being used for measurement, the CTD device must be ensured to be in good condition and functioning properly. Next, in figure (c), the ready CTD device will be attached to the pulley hook to be lowered to the bottom of the sediment and then raised back to the surface using the pulley system. Figure (d) provides a side view as the CTD is being inserted into the water for measurement. Then, figure (e) illustrates the fourth stage, which is when the CTD returns to the surface after completing the measurement, the CTD's rise will be slightly swayed due to the water pressure that requires adjustment. Finally, figure (f) shows the closing stage, where the CTD is placed on the side of the ship to dry first, checking the data that has been measured, checking the chart frame is confirmed to be intact and then also taking water samples from the niskin bottle, which will then be taken to the sediment laboratory for further analysis and the CTD tool will be dried and stored again.

In data recording, Midas Valeport brand CTD (Conductivity, Temperature and Depth) was used, which is a CTD tool produced by Teledyne Valeport (Pushidrosal, 2019), which is equipped with sensors to measure conductivity, temperature, pressure, and other parameters according to research needs. In this study, 5 niskin bottles were used to measure the parameters of temperature, salinity, conductivity, density and sound velocity through Direct-Reading data measurement, then controlled through the ship and operator, where the data will be automatically stored automatically into an integrated computer when the CTD starts to touch the water surface to the bottom sediment. This particular CTD observation research was carried out several times according to the station point and the possibility of free time, namely on March 11-30, 2019. At the observation of 1 station point, 1 trial of sinking the tool to the bottom sediment and returning to the surface to get the recording results (Pushidrosal, 2019).

The research method of data results starting from problem identification until completion is carried out in stages as attached in Figure 3.

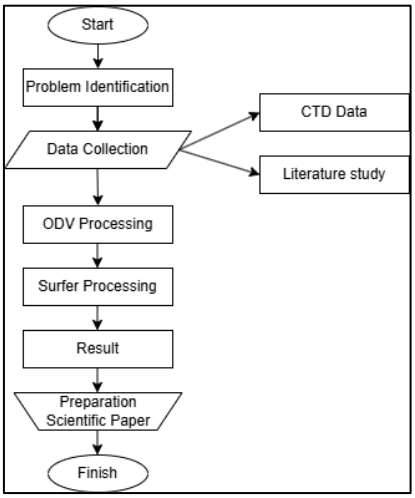

Figure 3. Author's Research Flow
(Source: Author, 2025)

Figure 3 explains the flow of data processing carried out by two processes, the first is data processing in ODV with the DIVA Gridding method, while data processing in Surfer uses the Kringing XYZ method. Both methods were chosen because they have the most detailed and refined result accuracy and can provide outputs that are in accordance with the research objectives. Data analysis begins with preprocessing, namely preparing primary and secondary data. Primary data is the data recorded by the CTD tool, while secondary data is supporting data from various literature sources and field reports. The primary data was then converted from VPD to XLSX format so that it could be processed using Ocean Data View (ODV). Processing in ODV software requires five main parameters, namely temperature, salinity, conductivity, density, and sound speed as well as longitude, latitude, and depth data. The processing results are displayed in the form of two-dimensional (2D) distributions as horizontal and vertical distributions. Then data processing using Surfer software, where in this tool only longitude and latitude data of each parameter are required. However, the Surfer software requires the separation of data per parameter in order to visualize the distribution pattern modeling of each parameter as needed. Furthermore, the two interpretation results from ODV and Surfer were analyzed to achieve the objectives of the study.

RESULT AND DISCUSSION

The following are the coordinates and description of the type of sediment present in each station as shown in Table 1.

Table 1. Coordinate Points of Observation Stations

NO.	POSITION													DESCRIPTION
	LATITUDE							LONGITUDE						
1	05	°	49	'	58,95	"	S	112	°	28	'	09.97	" E	MUD
2	05	°	49	'	59,35	"	S	112	°	25	'	35.68	" E	MUD
3	05	°	53	'	27,71	"	S	112	°	25	'	35.68	" E	SAND MUD
4	05	°	53	'	27,29	"	S	112	°	28	'	09.97	" E	SAND MUD
5	06	°	01	'	23,00	"	S	112	°	30	'	18.07	" E	SAND MUD
6	06	°	01	'	21,73	"	S	112	°	36	'	51.41	" E	SAND MUD
7	06	°	01	'	20,64	"	S	112	°	43	'	36.49	" E	SAND MUD
8	06	°	08	'	18,42	"	S	112	°	36	'	51.41	" E	SAND MUD
9	06	°	15	'	32,63	"	S	112	°	36	'	51.41	" E	SAND MUD
10	06	°	22	'	29,31	"	S	112	°	36	'	51.41	" E	SAND MUD

Source: Pusat Hidro Oseanografi TNI AL, 2019

The report shows that the sediment conditions at stations 1 and 2 are dominated by mud. Whereas at stations 3 to 10, the sediments found have sandy mud characteristics (Pushidrosal, 2019). To obtain more accurate analysis results, the approach used in this study was carried out systematically by dividing the research

data into three positions to see comparisons, namely horizontal, vertical, and 3D modeling of contour maps. This division aims to obtain a comprehensive understanding of parameter changes at the research site studied in the writing.

In the horizontal observation, analysis was conducted to identify parameter fluctuations based on different depths, namely at the surface, 20 meters depth, and 35 meters depth. Measurements at the surface layer were taken to obtain initial values, which were then compared with parameters at a depth of 20 meters as intermediate values. Meanwhile, a depth of 35 meters was chosen as a measurement point close to the bottom of the water sediment. Meanwhile, vertical observations were used to compare data between stations based on their proximity to the mainland of Bawean Island as a reference point. In this case, the observation points were grouped into three categories. The first group consists of station numbers 1, 2, 3, and 4 which are near the mainland and are hereafter referred to as stations near the mainland. The second group includes stations number 5, 6, and 7 which are farther away from the mainland, hence referred to as stations far from the mainland. The last group includes stations that form a pattern perpendicular to the coastline, namely station numbers 6, 8, 9, and 10. By far the best location for the marine environment is the far-land station group, because it is not affected by human activities from near land, and is also an ideal location because it does not extend straight into the open sea which allows the transition of thermal differences (Ningsih, et.al, 2022).

In addition, it is known that this research was conducted in March, which according to Hidayat, et.al, 2014, March is part of the first transitional season in Indonesia. This transitional season takes place during March, April and May (MAM) before entering the dry season. The selection of this period was considered based on climatological data used as secondary data in field research and obtained from the Meteorology, Climatology and Geophysics Agency (BMKG) Sangkapura Bawean Meteorological Station for the last 10 years (Pushidrosal, 2019). The decision to take measurements in March was also based on consideration of the more intensive environmental dynamics during this period. According to Pushidrosal, 2019, March coincides with the full moon phase, which causes tidal conditions to reach their maximum. This situation will certainly allow recording of more representative data related to fluctuations in the observed environmental parameters, so that the observation results can better describe the natural variations that occur at the research site.

A. Temperature Distribution Pattern

1. Temperature Horizontal Distribution Pattern

The horizontal temperature distribution is divided into 3 depths: surface, middle and bottom as shown in Figure 4.

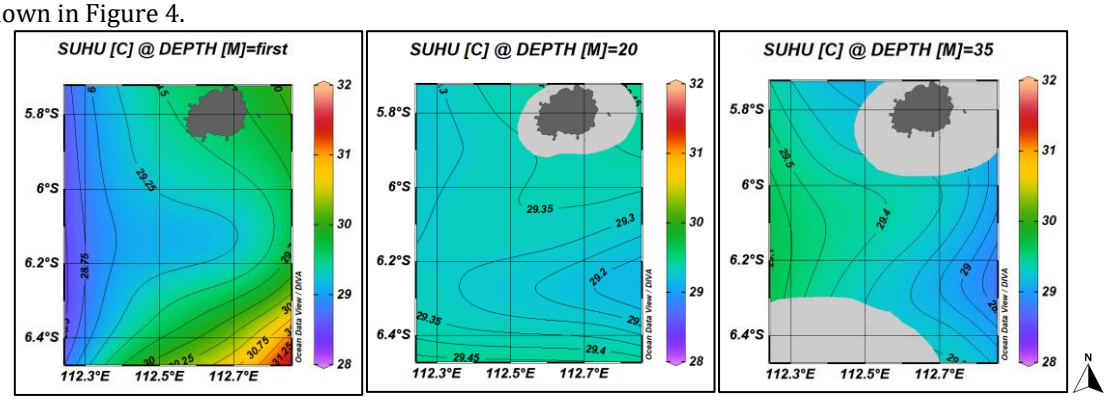

(a) (b) (c)

Figure 4. Temperature Horizontal Distribution (a=Surface, b=20 meters, c=35 meters)
(Source: Author, 2025)

Figure 4 (a) of surface temperature provides a visualization of quite varied changes, where higher temperatures are seen in the southeast, around 30.75°C-31.25°C, marked with yellow to orange colors. Then the temperature is lower in the northwest, around 28.75-29.25°C, marked in blue. This gradient shows the difference in heat distribution from external factors such as solar radiation, where the southeast region has a more optimal angle of irradiation than the western region because the data collection time is in the morning at 06.16 WIB (Pushidrosal, 2019), it can be categorized if exposure to more open rays increases the heat energy absorbed by the water surface in the southeast which has an impact on different but not significant temperature variations. In addition, variations in temperature distribution in the southeast region can also be analogized based on current patterns, according to field results from March 13 to April 11, 2019, it is known that the maximum current speed reached 0.594 m/s with high speed towards the Northeast to Southeast (Pushidrosal, 2019). This is certainly related between the distribution of temperature variations and current velocity, because the surface water mass in the western region will be pushed towards the northeast and southeast. This pushed warm water mass will cause an increase in temperature so that there is a buildup of warm water in the southeast.

Figure 4 (b) shows the temperature distribution at a depth of 20 meters, resulting in a

temperature range of 29.2°C-29.45°C. This distribution is certainly better than the surface, as seen from the more uniform contour lines. The more stable temperature indicates a better mixture of water masses compared to the surface. Then in Figure 4 (c), the temperature distribution at a depth of 35 meters, it appears that the distribution is increasingly homogeneous and close to the lowest value on the surface, indicating that deep waters have thermal characteristics that are much cooler and more stable. This theory is supported by research (Sidabutar, et.al, 2019) which states that seawater temperatures will continue to decrease with increasing depth due to a reduction in the intensity of sunlight entering the waters.

2. Temperature Vertical Distribution Pattern

The vertical distribution of temperature is divided into three groups as shown in Figure 5.

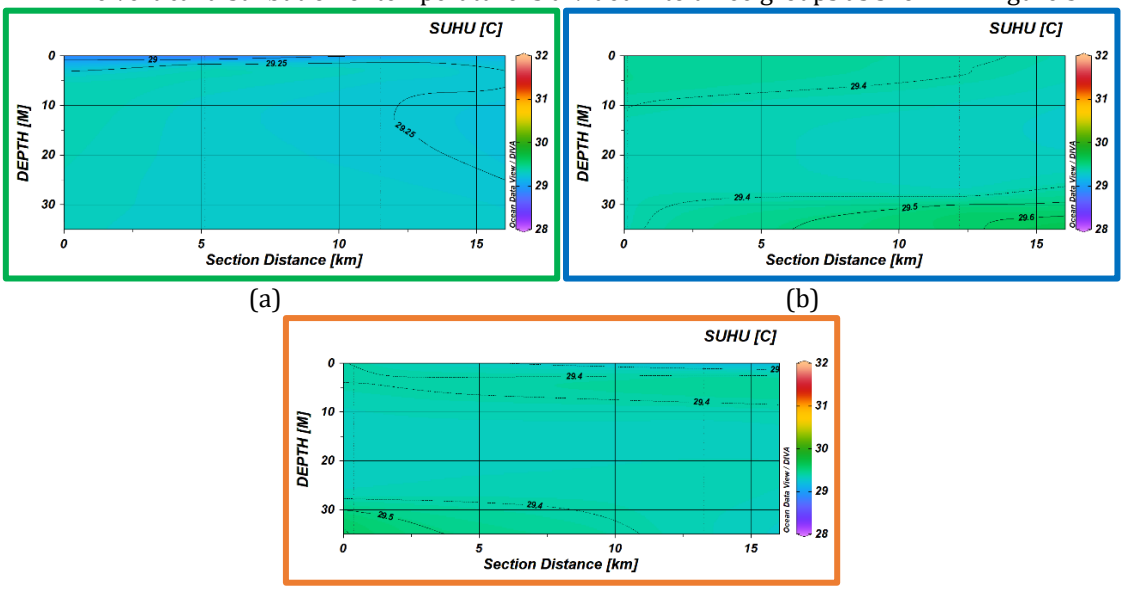

Figure 5. Temperature Vertical Distribution (a=Near Land, b=Far Land, c=Perpendicular to Land)

(Source: Author, 2025)

The results of Figure 5 (a), the temperature in the waters near the mainland shows a relatively lower value in the range of 29 ° C-29.25 ° C, especially at the surface there is a slightly lower temperature distribution compared to the next depth, this indication can be attributed to the location of the distance to the mainland which is classified as the closest so as to allow the influence of external factors such as the supply of fresh water from the estuary near the cooler land and have an impact on temperature changes that only occur at the top. This phenomenon is common as research conducted by (Prayogo, et.al, 2021) found the phenomenon of partially-mixed estuary or horizontal mixing of strong seawater with the water supply around the mainland. This is common in areas near land, especially in shallow water locations.

In Figure 5 (b), the temperature distribution at stations far from land, it appears that the temperature distribution tends to be more stable than the waters near land. Where at the surface it ranges from 29.4°C-29.6°C. This even distribution of relative temperature from the surface to the bottom indicates better vertical mixing. This more stable distribution can be indicated because of the lack of freshwater influence because it is located farther from land and also the impact of currents and upwelling which is more stable, thus increasing temperature homogeneity in the water column. In Tamayo's research, 2018, also obtained similar research results, explaining that the distant land area experienced more stable temperature fluctuations compared to the near-land area. This is due to the influence of local factors such as currents, upwelling, and freshwater input from the waters around the mainland.

Figure 5 (c) shows that the surface temperature at the station perpendicular to the mainland ranges from 29.4°C-29.5°C. Similar to the distant mainland, the distribution of temperature fluctuations at the station perpendicular to the mainland is also homogeneous due to the lack of influence of local factors near the mainland. Overall, when referring to the most stable condition of water temperature, the far mainland station category is a better temperature distribution point in terms of aquatic ecosystems. This is because the area has a stable, homogeneous temperature, and minimal influence of land or segmentation. According to Chen, et.al, 2024, states that marine environments that have stable and homogeneous temperatures tend to support healthier and more sustainable ecosystems.

3. Temperature Modeling and Contour Maps

To see the distribution pattern of the temperature parameter density, contour maps and modeling are needed as shown in Figure 6.

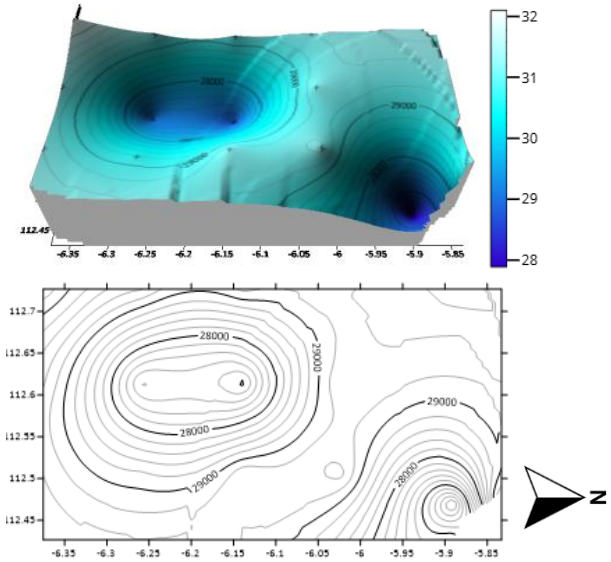

Figure 6. Temperature Distribution by 3D Modeling and Contour Map
(Source: Author, 2025)

The results of data visualization in Figure 6. display contour maps and 3D models of temperature distribution with cross sections that range the same as the range in ODV. The selection of this range was taken because it is in accordance with the general condition of water temperatures in Indonesia which generally ranges within these limits, as described in the study (Ramadani, et.al, 2022). From the 3D modeling results, two significant colors are visible that represent different temperature distribution patterns, marked by variations in color gradation. The dark blue zone signifies areas with tighter temperature contour changes, indicating temperature variation over shorter depth distances, while the light blue zone represents areas with more tenuous temperature changes.

If observed, the dark blue zone category is the station group area near the mainland and the station perpendicular to the mainland. Then for the light blue zone is the distant land station group. The difference in this phenomenon is in line with the vertical ODV results described earlier because the station near the mainland is influenced by upwelling and local activities around the waters, while the station perpendicular to the mainland is a thermal boundary area so that there are denser temperature changes but still homogeneous because of the absence of human activity from the mainland. As research by Ningsih, et.al, 2022 which explains the temperature gradient formed naturally as the transition of nearshore and perpendicular waters from the coast to the open sea will pass through a strong thermal boundary so that changes in parameters will generally occur more densely. Unlike the case with distant land which has more tenuous changes because there is no human activity and transverse against the direction of thermal fluctuations perpendicular to the land.

B. Salinity Distribution Pattern

1. Salinity Horizontal Distribution Pattern

The following visualization in Figure 7 visualizes the change in salinity horizontally.

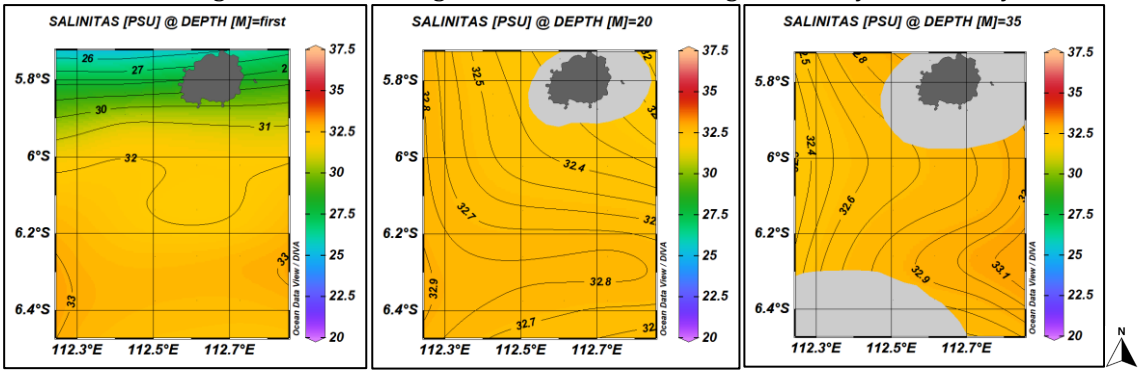

(c)

Figure 7. Salinity Horizontal Distribution (a=Surface, b=20 meters, c=35 meters)
(Source: Author, 2025)

When examining Figure 7 (a), which visualizes the distribution of surface depth salinity, it can be seen that there is a significant variation between the northern and southern parts of the water. In the north, salinity values are lower, ranging from 26-30 PSU, while in the south, salinity increases to 32-33 PSU. The northern area in the map shows lower salinity, which is due to the influence of the land having freshwater supply from the estuary causing water mass instrusion or freshwater intrusion from neighboring locations. In addition, when looking at the results of the previous report table data listed in Table 1. Coordinate Points of Observation Stations, it is known that station 1 and station 2 have muddy sediments and both are in the northern part. Supported by research from Lubayasari, 2010, states that muddy sediments have high porosity which allows longer freshwater retention, thus reducing salinity in the area.

Therefore, the surface salinity in the north is relatively smaller in variation compared to other areas. At a depth of 20 meters in Figure 7 (b), the salinity distribution becomes more uniform compared to the surface layer which is between 32.4-32.9 PSU. Then figure 7 (c) presents the salinity distribution at a depth of 35 meters, the salinity appears to be more stable in the range of 32.4-33.1 PSU. The absence of sharp gradations at this depth as well as gradations in the surface layer, indicates that external factors such as freshwater supply, runoff from land are more dominant in the upper layer compared to 35 meters depth.

2. Salinity Vertical Distribution Pattern

The distribution of salinity is visualized in Figure 8 below.

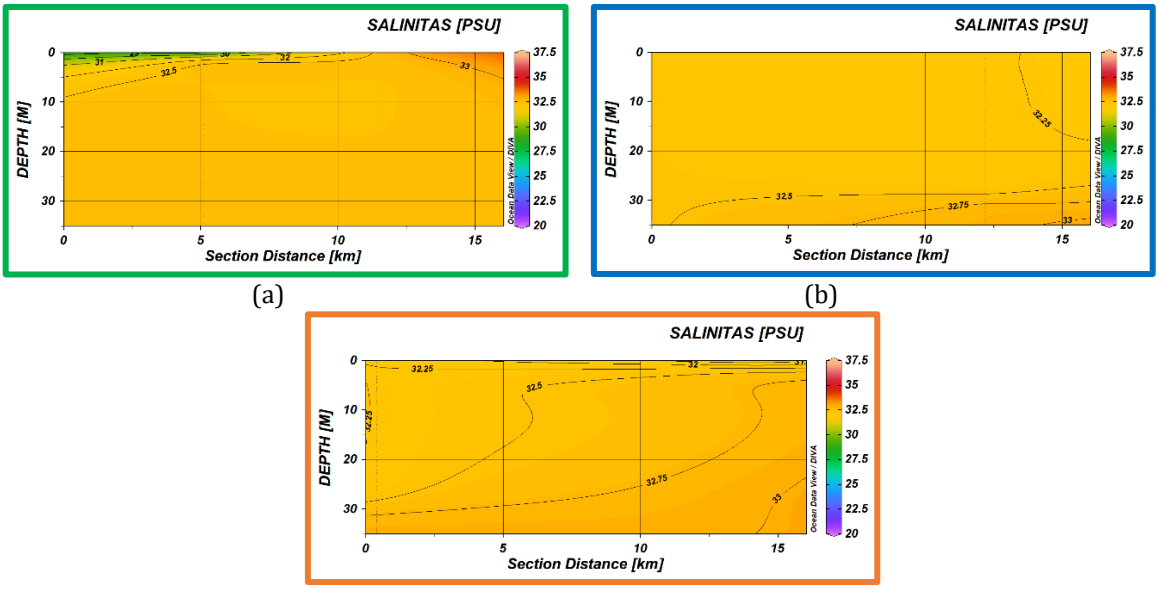

Figure 8. Salinity Vertical Distribution (a=Near Land, b=Far Land, c=Perpendicular to Land)
(Source: Author, 2025)

Figure 8 (a). The surface layer shows a slight decrease in salinity due to the possibility of freshwater input from the mainland or called water mass intrusion, which is an influence caused by the entry of a type of water mass in one area into another area that exerts influence. It appears in the picture for the surface part further to the right, which means that the further away from the mainland, the higher the salinity. According to research from Haidar, 2021, explaining the influx of other water causes salinity to tend to be higher on the side closer to the sea.

In figure (b) the salinity distribution away from land appears uniform with a range of 32.25-33 PSU. There is no mixing of freshwater so that it can show the dominance of a more stable sea water mass. Furthermore, figure (c) presents an image of the distribution of salinity perpendicular to the mainland with a range of 32-33 PSU. The deeper the salinity value increases with a continuous increase of 0.25 PSU, this is common because the deeper it is, the closer it is to sediment deposits containing high salinity levels (Maharani, et.al, 2014).

3. Salinity Modeling and Contour Maps

The contour maps and modeling distribution is visualized through figure 9 as below.

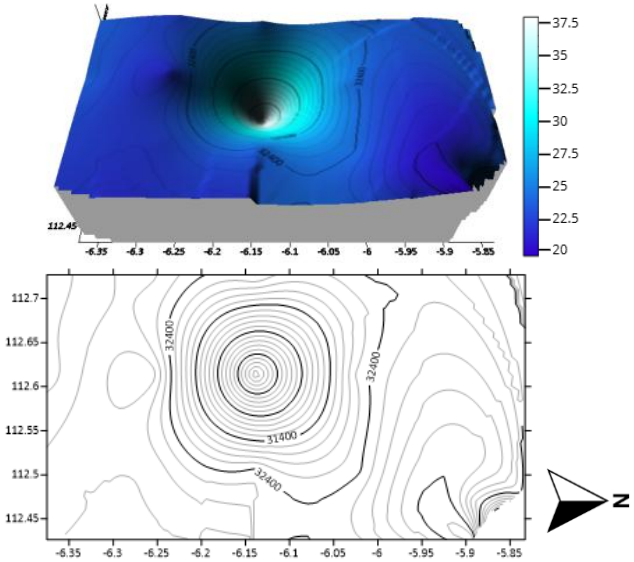

Figure 9. Salinity Distribution by 3D Modeling and Contour Map
(Source: Author, 2025)

From the visualization of Figure 9, there is a low salinity center located perpendicular to the mainland and near the mainland. The results of contour line visualization and salinity modeling have a cause and effect with the analysis results in the previous temperature parameter modeling. It is known that the temperature is denser in the same two groups, so the salinity results will contradict each other. In accordance with the research of Patty, et.al, 2023, explained that the distribution of salinity has an inversely proportional nature to temperature, so that when the temperature decreases, salinity tends to increase, and vice versa. So in this modeling, it can be analyzed that the location of the group that has a tight temperature will be a tenuous salinity result.

C. Conductivity Distribution Pattern

1. Conductivity Horizontal Distribution Pattern

As Figure 10 shows, the conductivity pattern is horizontally distributed.

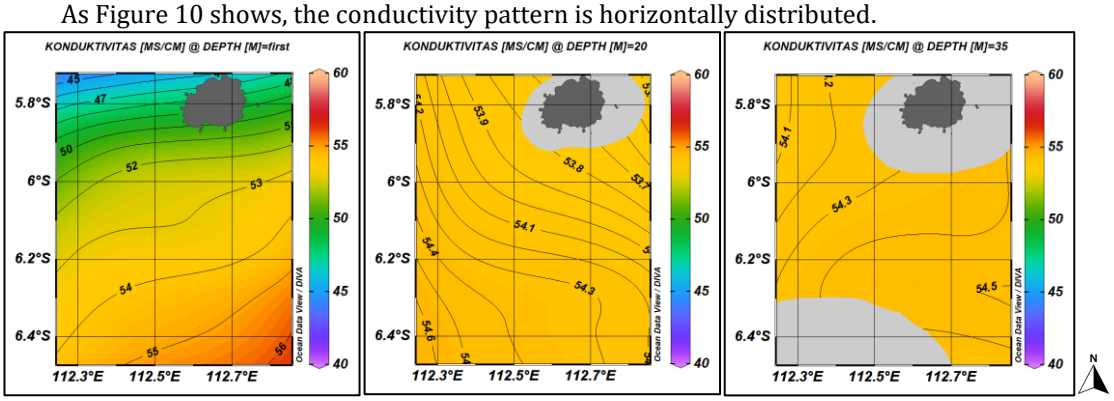

(a) (b) (c)

Figure 10. Conductivity Horizontal Distribution (a=Surface, b=20 meters, c=35 meters)
(Source: Author, 2025)

Figure 10 (a) shows that the conductivity of the northern part is 45-50µS/cm compared to 56 µS/cm in the southern part. There is a gradation of change from north to south. This is related to the results of the previous parameter analysis regarding salinity in the north which has a lower value in the surface layer. Lower salinity will certainly reduce the level of conductivity as well. The northern surface is affected by land so that the instrusion of water masses will make seawater fresher so that it has less ion content than saltier water, as well as similar research from (Prihatno, et.al, 2021) which explains the relationship between salinity and conductivity parameters which are unidirectional.

Figure 10 (b) shows that the conductivity at a depth of 20 meters shows an increase compared to the surface, with an average value of 53.7-54.6 µS/cm. So it can be indicated that the water at this

depth is more homogeneous in physicochemical properties. Figure 10 (c) shows that the conductivity at 35 meters depth is stable with a range of 54.1-54.5 µS/cm, which is judged from the effect of depth mixing starting to be more dominant, so the conductivity increases.

2. Conductivity Vertical Distribution Pattern

A visual display of the vertical distribution of conductivity is presented in Figure 11.

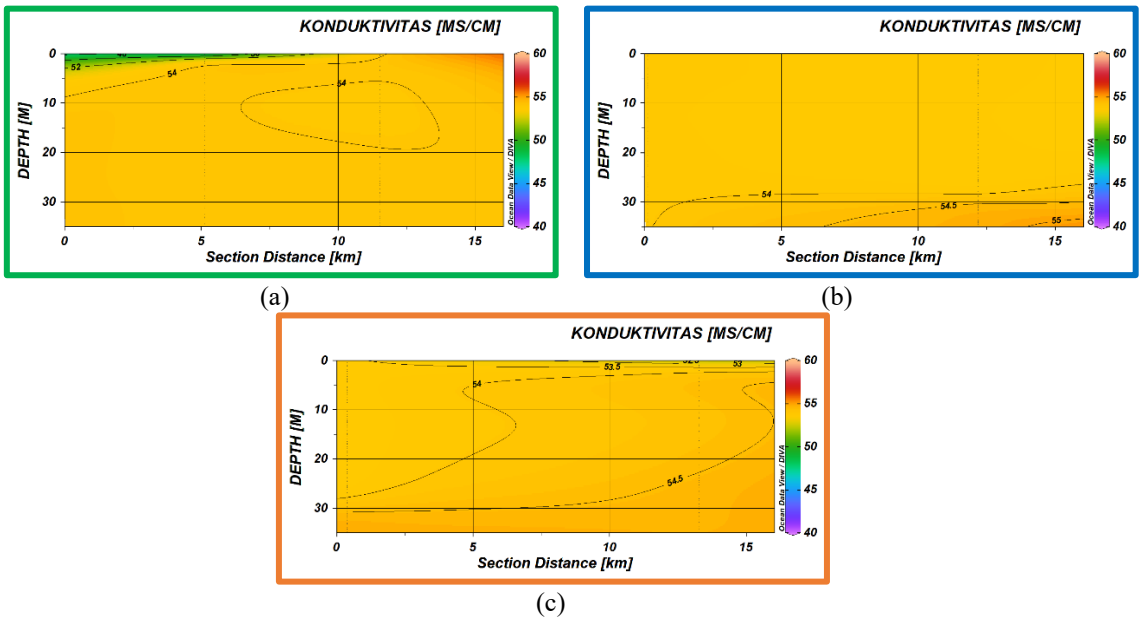

Figure 11. Conductivity Vertical Distribution (a=Near Land, b=Far Land, c=Perpendicular to Land)

(Source: Author, 2025)

Figure 11 (a) surface conductivity is 52-54 µS/cm. In deeper areas the results stabilized at 54 µS/cm. The uneven distribution of conductivity indicates the mixing of freshwater given the proximity to land. The influence of freshwater from land causes lower conductivity at the surface only because estuary flow carries water with lower conductivity so that a vertical gradient can occur. This phenomenon is common in areas near land. A similar thing was also found (Fahimah, et.al, 2021), in their research, they mentioned that the mixing of freshwater from land that has a lower conductivity will create a vertical gradient. If you look at Figure 11 (b), the conductivity tends to be more stable, with a value of 54-55 µS/cm evenly distributed. There appears to be no significant change at the surface like the stations near land and the isochonductivity distribution pattern shows better mixing of water masses. Whereas in Figure 11 (c) the surface conductivity is relatively variable, between 53-54.5 µS/cm.

3. Conductivity Modeling and Contour Maps

The distribution pattern of conductivity parameter density is visualized in Figure 12.

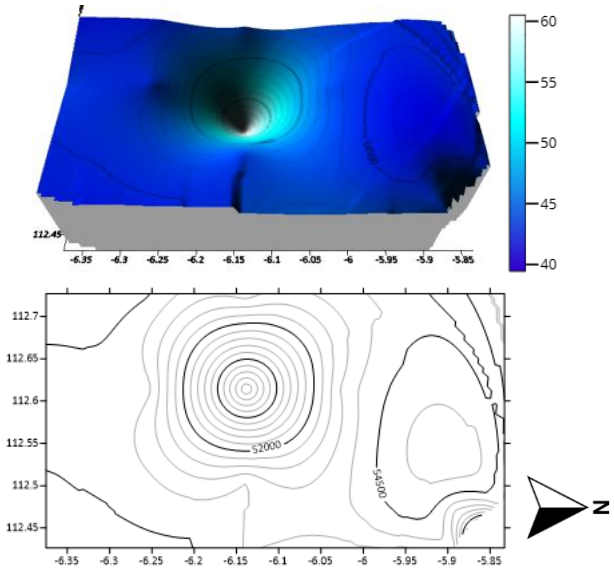

Figure 12. Conductivity Distribution by 3D Modeling and Contour Maps

(Source: Author, 2025)

Water conductivity is the ability of water to conduct electricity which depends on the amount of dissolved ions such as salt, therefore the results of conductivity data processing are similar in pattern to salinity. Said by Prihatno, et.al, 2021, explaining that the higher the salinity, the higher the dissolved mineral content, which contributes to an increase in conductivity or electrical conductivity. In the results, the conductivity values obtained ranged from 52-54.5 µS/cm. The areas with denser conductivity distribution are located perpendicular to the mainland and slightly near the mainland.

D. Density Distribution Pattern

1. Density Horizontal Distribution Pattern

Figure 13 illustrates the horizontal temperature distribution.

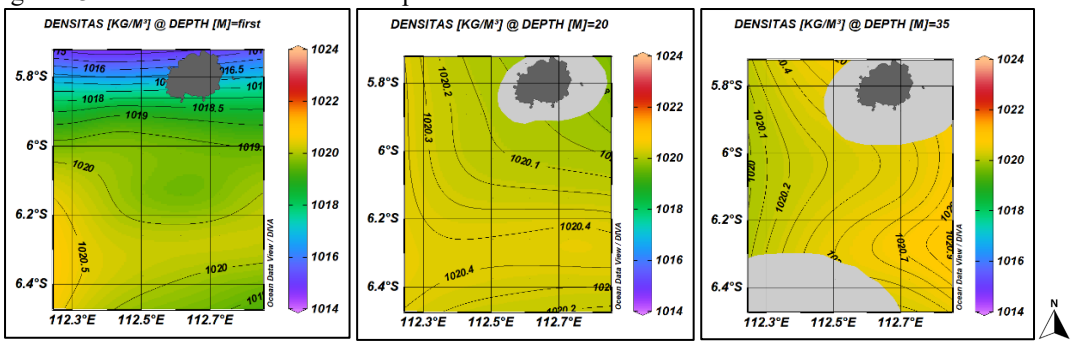

(a) (b) (c)

Figure 13. Density Horizontal Distribution (a=Surface, b=20 meters, c=35 meters)

(Source: Author, 2025)

Based on Figure 13 (a) regarding the visualization results on density on the surface, it can be seen that at this location the density levels tend to be lower in the northern part around 1016-1019 kg/m^3. Then the density level increases towards the south with a value reaching 1020-1020.5 kg/m^3. This is in line with the results of the previous parameter, salinity. Where salinity is low in the north, therefore the density results in the north are also low because water molecules tend to be looser. As in previous studies that conducted research on the relationship between temperature, salinity and density. In his analysis, Pawlowicz, 2013, explained that higher salinity will have a greater mass, and therefore will be denser or higher density, and vice versa.

Then Figure 13 (b) which presents the density distribution with a depth of 20 meters shows a more stable density level when compared to the surface in the range of 1020.1-1020.4 kg/m^3, or it can be said that the distribution is homogeneous. While in Figure 13 (c), namely the distribution of density parameters at a depth of 35 meters, it appears that the results of higher density levels are in the range of 1020-1020.7 kg/m^3, this can occur due to the influence of the depth which is also getting deeper. Supported by research by Maharani, et.al, 2014 mentioned that the density of seawater will increase with increasing depth, because higher salinity increases the mass of water without increasing its volume.

2. Density Vertical Distribution Pattern

Figure 14 shows the difference in density based on the vertical direction.

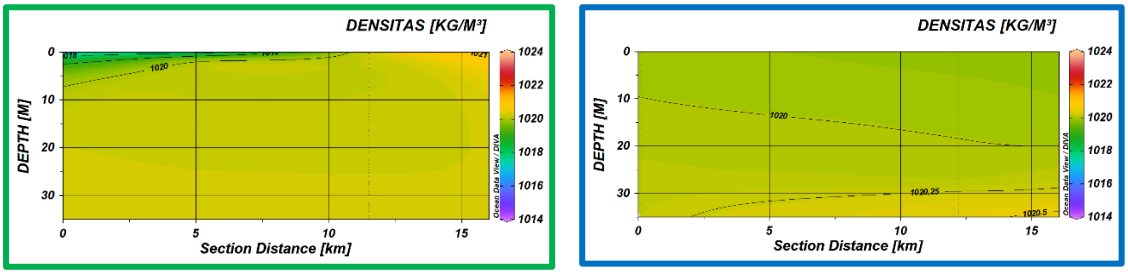

(a) (b)

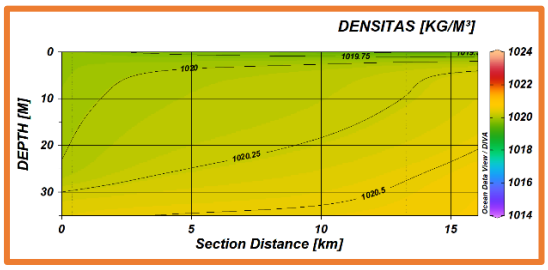

(c)

Figure 14. Density Vertical Distribution (a=near land, b=Far Land, c=Straight Land)
(Source: Author, 2025)

Figure 14 (a) density distribution of stations near the mainland shows that the surface density results are in the range of 1018-1021 kg/m^3. There is a slight increase in the variable fluctuations that occur at the surface between those that are very close to the mainland and those that are more distant from the mainland. As research by Howart, et.al, 2014 explains, density gradients at the surface can indeed vary spatially, with small differences between areas very close to land and those slightly further away. This is due to the influence of freshwater inflow from land that affects salinity and temperature, thus affecting seawater density as well.

Figure 14 (b) of the distant land station shows relatively uniform density results of around 1020-1020.5kg/m^3, due to the lack of influence of external factors. While in Figure 14 (c), the station group perpendicular to the mainland is almost uniform, which ranges from 1020-1020.5 kg/m^3 with a difference increasing by 0.25 kg/m^3 as depth.

3. Density Modeling and Contour Maps

Figure 15 shows the density distribution in the form of contour maps and modeling.

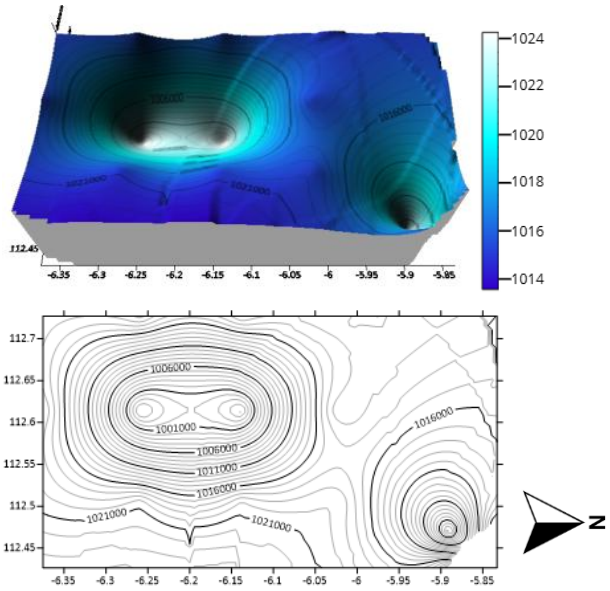

Figure 15. Density Distribution by 3D Modeling and Contour Maps
(Source: Author, 2025)

Density or density of seawater is a fundamental parameter that determines the level of water density in a location, also known as water mass density (Grekov, et.al, 2021). Based on the visualization results of Figure 15, the distribution of density and temperature shows an opposite pattern. Where if in the temperature modeling results there is a tighter distribution pattern in the station group near the mainland and perpendicular to the mainland, the visualization results of density modeling occur stretching in both locations. This phenomenon is in accordance with the theory of fluid physics which states that when the temperature is low or denser, the density decreases due to water molecules arranged more slowly and stretching each other, otherwise at hotter temperatures, water experiences thermal expansion (Makoto, 2015).

E. Sound Speed Distribution Pattern

1. Sound Speed Horizontal Distribution Pattern

The following visualization results of the horizontal distribution of sound velocity are presented in Figure 16.

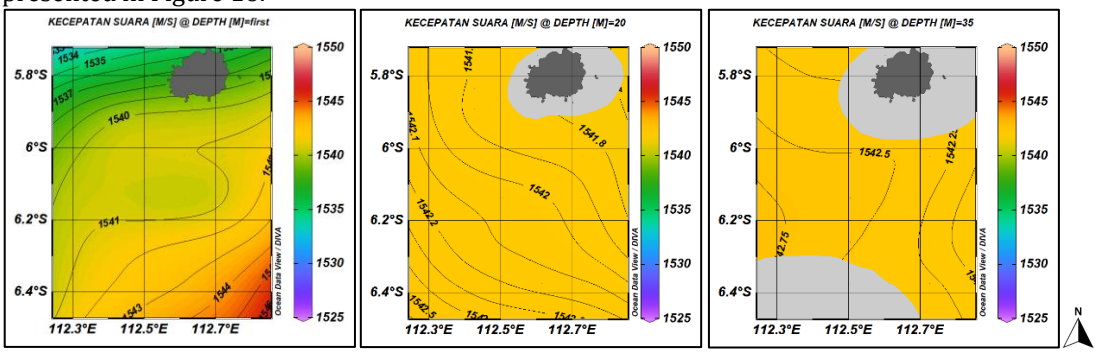

(a) (b) (c)

Figure 16. Sound Speed Horizontal Distribution (a=Surface, b=20 meters, c=35 meters)
(Source: Author, 2025)

Figure 16 (a) contains the distribution of sound speed at the surface at 1534 m/s-1546 m/s and there are variations in two spatial distributions, namely in the southeast region the sound speed is higher around 1544 m/s-1546 m/s, while the northwest region has a lower sound speed, around 1534 m/s-1540 m/s. This sound speed parameter is most closely related to the temperature parameter as Medwin's empirical evidence of the influence of temperature and sound speed (Lubis, et.al, 2015). Previous visual temperature results also showed warmer temperatures in the southeast. The increase in temperature causes molecular expansion that increases the speed of sound propagation. The role of ocean currents also contributes, thus pushing the warm water mass from the west to the southeast and increasing the speed of sound in the area. Furthermore, in Figure 16 (b), the depth of 20 meters, the range of sound speed values is at 1541.8 m/s-1542.5 m/s with a homogeneous distribution. If you look at the results of the temperature parameters at this depth, it is more stable, namely 29.2 ° C-29.45 ° C so that changes in sound velocity will definitely be more constant, supported by pressure based on depth. Then in Figure 16 (c) the range of sound velocity values ranges from 1542.25 m/s-1542.75 m/s with a homogeneous distribution compared to the previous two layers.

2. Sound Speed Vertical Distribution Pattern

In Figure 17, three types of vertically varying velocity distributions are shown.

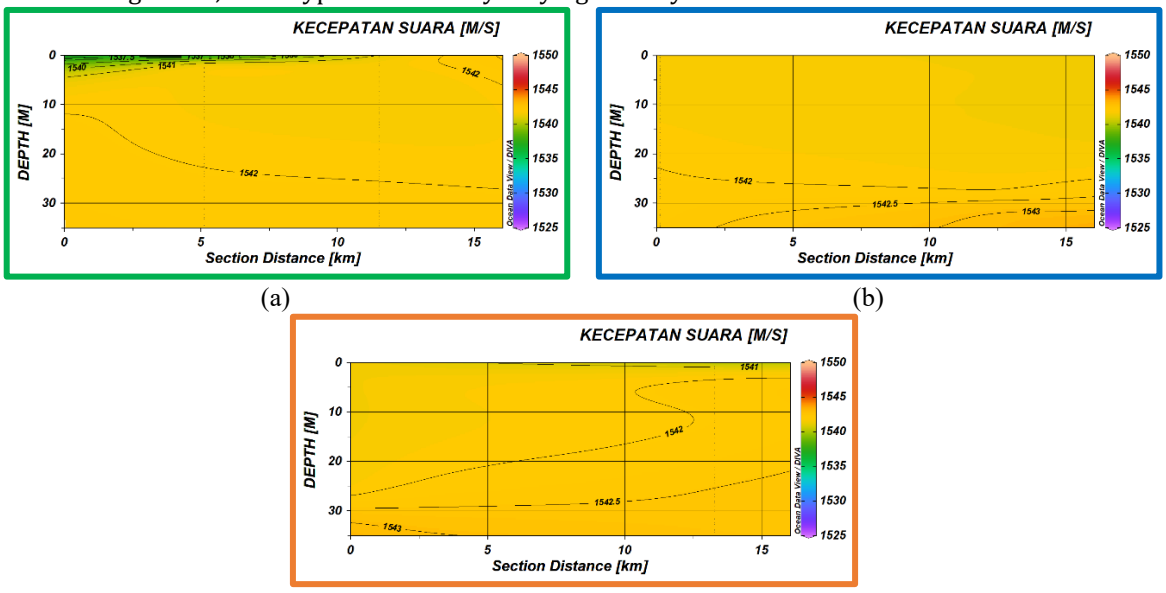

(a) (b)

(c)

Figure 17. Sound Speed Vertical Distribution (a=Near Land, b=Far Land, c=Straight Land)
(Source: Author, 2025)

The sound speed is relatively lower at the surface, ranging from 1537.5-1542 m/s and gradually increases with depth. As stated in the study of Frosch, 1996, said that the variation of sound velocity in the deep sea is influenced by the almost constant temperature and increased pressure, causing the sound velocity to increase along with the depth. Figure (b) is a station far inland showing a more stable

and homogeneous sound speed. At the top, the sound speed values range from 1542-1543 m/s, showing a uniform distribution pattern. Then in figure (c) the station perpendicular to the mainland which is a station with a transition path between nearshore waters and offshore waters, so that the distribution pattern has mixed characteristics of the two previous areas. The sound speed in this area ranges from 1541-1543 m/s.

3. Sound Speed and Modeling Contour Maps

Figure 18 Sound speed distribution pattern in contour map and modeling.

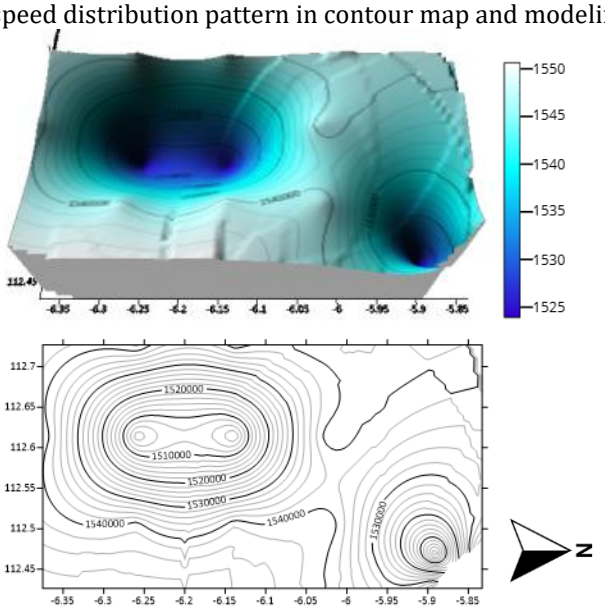

Figure 18. Sound Speed Distribution by 3D Modeling and Contour Map
(Source: Author, 2025)

Figure 18. describes the density distribution pattern of the sound speed parameter, where the sound speed is a parameter that determines how fast sound waves are able to propagate through the seawater medium. This parameter is generally influenced by temperature. In accordance with the theory of sound propagation in water, at low temperature conditions, the sound speed will also be low. This happens because water molecules have kinetic energy, so sound waves propagate at a smaller speed. However, with increasing depth, the speed of sound can be compressed and increased due to the role of water pressure as this theory is applied to special submarines (Lubis, et.al, 2015).

CONCLUSION

1. The horizontal and vertical distribution patterns using Ocean Data View (ODV) software, the temperature of Bawean Waters is in the range of 28.75°C-31.25°C. Salinity showed a variation of 26 PSU-33.1 PSU. Conductivity parameters range in the range of 45-55 µS/cm. Seawater density has values between 1016-1021 kg/m^3. The speed of sound is between 1534-1543 m/s. In addition, the results of mapping horizontal and vertical distribution patterns provide an understanding that depth has an influence on changes in oceanographic parameter values. There is a difference in concentration between the surface, middle, and bottom layers of the water.
2. Parameter CTD distribution pattern through contour map analysis and 3D modeling. In the visualization, there are two different results in the form of light blue zones and dark blue zones that describe areas with dense and sparse parameter density distribution patterns.

REFERENCES

Amri, K., Ma'mun, A., & Taufik, M. (2021). Oceanographic Characteristics of the Western Banda Sea in the Western Season from 2016 In-Situ Measurement Data. Journal of Applied Marine and Fisheries (JKPT), 4(1), 1-11.

Djumanto, D. (2010). Spatial Distribution of Plankton in Bawean Waters. Fisheries Journal *Universitas Gadjah Mada*, *12*(1), 43-49.

Fahimah, N., Damayanti, A. D., Bunga, V. U., & Mubiarto, H. (2021). Vertical and Horizontal Profiles of Salinity, DHL, and Tds Parameters Based on Seasonal Variations in the Citarum River Estuary. Oceanana, 46(1), 1-12.

Ferriska, O. (2017). Bathymetric Survey in Shallow Waters Using USV (Unmanned Surface Vehicle), HIMAGE USV I (Doctoral Dissertation, Institut Teknologi Sepuluh Nopember).

Ferriska, O. (2017). Bathymetric Survey in Shallow Waters Using USV (Unmanned Surface Vehicle), HIMAGE USV I (Doctoral Dissertation, Institut Teknologi Sepuluh Nopember).

Frosch, R. A. (1964). Underwater Sound: Deep-Ocean Propagation: Variations Of Temperature And Pressure Have

Great Influence On The Propagation Of Sound In The Ocean. Science, 146(3646), 889-894.
Grekov, A. N., Grekov, N. A., & Sychov, E. N. (2021). Measuring Salinity And Density Of Seawater Samples With Different Salt Compositions And Suspended Materials. Metrology, 1(2), 107-121.
Haidar, A. Z., Handoyo, G., & Indrayanti, E. (2021). Horizontal Distribution of Salinity in the Estuary of Bondet River, Cirebon, West Java. Journal of Marine Research, 10(2), 275-280.
Hatta, M. (2014). Relationship between Oceanographic Parameters and Chlorophyll-A Content in the Eastern Season in the Northern Waters of Papua. Torani Journal Of Fisheries And Marine Science, 24(3).
Hidayat, R., & Ando, K. (2014). Indonesian Rainfall Variability and Its Relationship with ENSO/IOD: Estimation Using JRA-25/JCDAS Data. Agromet, 28(1), 1-8.
Hermansyah, H., Atmadipoera, A. S., Prartono, T., Jaya, I., & Syamsudin, F. (2021). Turbulent Mixing in the Sulawesi Sea Using Thorpe Analysis Estimation. Journal of Tropical Oceanography, 24(2), 211-222.
Herwindya, A. Y., Febriawan, H. K., Nugroho, A. B., & Dannari, A. (2020). Hydro-Oceanographic Survey in Raja Ampat Waters, West Papua, Indonesia. Oceanika, 1(2), 48-64.
Hidayah, Z., Wirayuhanto, H., Sari, Z. R. N., & Wardhani, M. K. (2021, November). Modeling Sea Surface Currents In The Eastern Coast Of Bawean Island, East Java. In IOP Conference Series: Earth And Environmental Science (Vol. 925, No. 1, P. 012006). IOP Publishing.
Howarth, M. J., Balfour, C. A., Player, R. J., & Polton, J. A. (2014). Assessment Of Coastal Density Gradients Near A Macro-Tidal Estuary: Application To The Mersey And Liverpool Bay. Continental Shelf Research, 87, 73-83.
Lubayasari, W. D. (2010). Spatial Distribution Patterns and Population Dynamics of Blood Clams (Anadara Granosa, L) in the Waters of Lada Bay and Banten Bay, Banten Province.
Lubis, M. Z., Silaban, R. D., Siboro, A. T., Siahaan, F. A. G., & Anurogo, W. (2018). Influence of Oceanographic Conditions on Climate Change in Batu Ampar Waters, Riau Islands. Journal of Marine Science: Indonesian Journal Of Marine Science And Technology, 11(2), 191-199.
Lubis, M. Z., Surya, G., Anggraini, K., & Kausarian, H. (2017). Application of Hydroacoustic Technology in the Field of Marine Science and Technology. Oseana, 42(2), 34-44.
Maharani, W. R., Setiyono, H., & Setyawan, W. B. (2014). Study of Vertical and Horizontal Distribution of Temperature, Salinity and Density in Coastal Waters, Probolinggo, East Java. Journal of Oceanography, 3(2), 151-160.
Muhaemin, M., Arifin, T., Mahdafikia, N., & Fihrin, H. (2022). Influence of Physical Oceanographic Parameters on Indications of Coral Bleaching in Kapoposang Spermonde Marine Tourism Park (TWP) Makassar Strait. Journal of Marine Research, 11(4), 587-597.
Mutmainnah, N., Asyiah, I. N., & Novenda, I. L. (2021). Utilization of Traditional Fishing Gear by Bawean Island Fishermen in Gresik Regency. Journal of Tropical Fisheries, 8(1), 23-34.
Ningsih, E. N., Agussalim, A., Barrus, S., & Hartoni, H. (2024). Spatio-temporal variability of sea surface temperature in coastal part of Banyuasin Regency, South Sumatra Province. JOURNAL ENGGANO, 9(1), 1-10.
Patty, S. I., & Huwae, R. (2023). Temperature, Salinity And Dissolved Oxygen West And East Seasons In The Waters Of Amurang Bay, North Sulawesi. Platax Scientific Journal, 11(1), 196-205.
Pawlowicz, R. (2013). Key physical variables in the ocean: temperature, salinity, and density. Nature Education Knowledge, 4(4), 13.
Prayogo, L. M., & Kurniawan, I. A. (2021). Study of Physical and Chemical Oceanographic Parameters in Sulawesi Island Waters, Indonesia. Journal of Tropical Marine Research (J-Tropimar), 3(1), 12-23.
Prihatno, H., Abida, R. F., & Sagala, S. L. (2021). Correlation between Seawater Conductivity and the Amount of Dissolved Minerals in the Madura Strait Waters. National Marine Journal, 16(3), 211-222.
Rey Avila Mangarin, D. K. J. T. (2024). Teaching Business Concepts Effectively: A Desk Research Approach.
Rienetza, A. Z., Zahrina, N., Yanfeto, B., & Agassi, R. N. (2023). 2D Tidal And Wave Modeling Using Numerical Method With Flow Model And Spectral Wave Mike 21 Software In The Waters Of Tanjung Mulang To Meru Bay In January . Indonesian Hydrographic Journal, 5(2), 57-66.
Robles-Tamayo, C. M., Valdez-Holguín, J. E., García-Morales, R., Figueroa-Preciado, G., Herrera-Cervantes, H., López-Martínez, J., & Enríquez-Ocaña, L. F. (2018). Sea Surface Temperature (SST) Variability Of The Eastern Coastal Zone Of The Gulf Of California. Remote Sensing, 10(9), 1434.
Schlitzer, Reiner. "Ocean Data View." (2022).
Senduk, N. (2021). Application of Contour Line Drawing Technique Using Auto Cad 3D. Journal of Applied Civil Engineering, 3(2), 90-100.
Setiyo Pranowo, W., Nurhidayat, N., & Asmoro, N. W. (2022). Characteristic Of Temperature And Salinity In The Makassar Strait Based On CTD Cruise Arlindo 2005 And Timit 2015 Data: Characteristic Of Temperature And Salinity In The Makassar Strait Based On Arlindo 2005 And Timit 2015 CTD Cruise Data. Journal of Chart Datum, 8(2), 107-116.
Soesanto, E., Rasyid, A., & Suyanto, H. (2022). Offshore Design Planning of Subsea Construction Using Geophysical Modeling Data Processing with Surfer 3D Simulation Program. Journal of Bhara Petro Energi, 37-46.
Williams, A. (2009). CTD (Conductivity, Temperature, Depth) Profiler. Encyclopedia Of Ocean Sciences:

Measurement Techniques, Sensors And Platforms, 25-34.
Xiao, S., Zhang, M., Liu, C., Jiang, C., Wang, X., & Yang, F. (2023). CTD Sensors For Ocean Investigation Including State Of Art And Commercially Available. Sensors, 23(2), 586.
Yasutomi, M. (2015). Thermodynamic Mechanism Of The Density Anomaly Of Liquid Water. Frontiers In Physics, 3, 8.
Yuliardi, A. Y., Prayogo, L. M., & Joesidawati, M. I. (2022). Dynamics of the Spatial-Vertical Distribution of Water Masses in the West and East Indonesian Throughflow Routes in the Wet Season. Miyang Journal: Ronggolawe Fisheries and Marine Science Journal, 2(2), 38-46.